International Journal of Greenhouse Gas Control 14 (2013) 220–226

Contents lists available at SciVerse ScienceDirect

International Journal of Greenhouse Gas Control

journal homepage: www.elsevier.com/locate/ijggc

Evidence of irreversible CO_2 intercalation in montmorillonite

Vyacheslav N. Romanov*

National Energy Technology Laboratory, P.O. Box 10940, Pittsburgh, PA 15236, United States

ARTICLE INFO

Article history:
Received 6 November 2012
Received in revised form 11 January 2013
Accepted 14 January 2013

Keywords:
Clay
Carbon dioxide
Sorption
Spectroscopy
XRD

ABSTRACT

Mitigation of the global climate change via sequestration of anthropogenic carbon dioxide (CO_2) in geologic formations requires assessment of the reservoir storage capacity and cap rock seal integrity. The typical cap rock is shale or mudstone rich in clay minerals that may significantly affect the effectiveness of the CO_2 trapping. Specific objectives of this study were to conduct experimental investigation into the processes associated with CO_2 and H_2O trapped in swelling clay, namely, Wyoming and Texas montmorillonite powder. Combined (same-sample) multi-technique data – manometric sorption isotherm hysteresis, diffuse reflectance infrared spectroscopy 'trapped CO_2' fingerprints, irreversible X-ray diffraction patterns for the clay interlayer in intermediate hydration state, and HF acid digestion resulting in formation of non-extractable F:CO_2 adducts – corroborate a hypothesis that carbon dioxide molecules can be irreversibly trapped via anomalous extreme confinement in the galleries associated with montmorillonite interlayer, which may result in formation of carbonates in the longer term. Validation on Arizona montmorillonite lumps substantiated the evidence that such processes may occur in natural clay deposits but possibly on a different scale and at a different rate.

Published by Elsevier Ltd.

1. Introduction

Sequestration of greenhouse gases (GHGs) in geologic formations is a viable approach to mitigation of the global climate change. Options for geologic storage of anthropogenic carbon dioxide (CO_2) vary from saline aquifers and depleted oil and gas fields to unmineable coal seams (DOE/NETL, 2010). Important consideration is potential changes in caprock seal integrity, owing to interaction with CO_2. The typical caprock is shale or mudstone rich in clay minerals that may significantly affect the effectiveness of CO_2 trapping. Swelling clay minerals, such as smectite with aluminosilicate structure controlled by low-charge layers, can accommodate water and, potentially, carbon dioxide molecules in the interlayer region (Romanov et al., 2009a; Knudson and McAtee, 1973).

Dioctahedral smectites have a 2:1 lamellar structure with an octahedral sheet of repeating AlO_6 units sandwiched between two tetrahedral silicate (SiO_4) sheets. Isomorphic metal-ion substitutions in either layer (*e.g.*, Al^{3+} replaced by Mg^{2+} or Fe^{2+} in the octahedral sheet or Si^{4+} replaced by Al^{3+} in the tetrahedral sheet) result in fixed-charge imbalance that is compensated by metal cations (*e.g.*, Na^+ or Ca^{2+}) residing at or near the clay surfaces. The lamellae, thus held together by electrostatic forces, can be expanded by penetration of polar (or polarizable) molecules into the interlayer (Romanov et al., 2009a; Ferrage et al., 2005). Heterogeneity of smectites can lead to coexistence of layers with substantially different degrees of hydration, within the same crystallite (Ferrage et al., 2005).

Original debates around the CO_2 intercalation hypothesis stemmed from interpretations of the B.E.T. (Brunauer et al., 1938) surface area measurements on cation-exchanged montmorillonites, related to differences in sample preparation, sensitivities of cryogenic (−78 °C) adsorption apparatus, and theoretical assumptions with regard to organization of the lamellae in the clay matrix being affected by the cation exchange, dialysis, and drying procedures (Thomas et al., 1970). The first report that CO_2 can penetrate the interlamellar space of Cs-smectite (Thomas and Bohor, 1968) was initially challenged, on the grounds of scientific merit, by Aylmore et al. (1970) but was later re-affirmed by Fripiat et al. (1974), based on additional evidence using an infrared (IR) transmission spectrometer (at room temperature and −78 °C) and X-ray goniometer (20 °C to −70 °C to 20 °C) experiments on the same clays that were used by Thomas and Bohor (1968). Despite the very low CO_2 pressure (<1 atm.) used in their work, Fripiat et al. (1974) reported noticeable orientation dependency of the asymmetric stretching (ν_3) band in the 2350 cm^{-1} region of the absorbed IR spectra of K- and Cs-smectite and significant swelling of Na- and Ca-smectite due to CO_2 condensation during the cooling cycle. Interestingly, the changes in d_{001} spacing were reversible in both Na-exchanged (10.0 Å to 12.3 Å to 10.0 Å) and Ca-exchanged (13.2 Å to 14.2 Å to 13.2 Å) smectites but the

* Corresponding author. Tel.: +1 412 386 5476; fax: +1 412 386 4604.
E-mail address: romanov@netl.doe.gov

1750-5836/$ – see front matter. Published by Elsevier Ltd.
http://dx.doi.org/10.1016/j.ijggc.2013.01.022

changes in d_{002} and d_{003} peak positions appeared to be irreversible with the Ca-smectite. The IR spectra of Na- and Ca-smectites were not reported. Later, Fahmy et al. (1993) observed that the magnitude of saturated swelling of Mg-montmorillonite clay is not monotonically dependent on CO_2 pressure at 45 °C, which they attributed to a competition between the swelling caused by increasing solubility of added water in CO_2-rich phase and the hydrostatic pressure compaction effect but the exact mechanisms were not understood.Molecular-scale phenomena related to CO_2 interaction with swelling clays have recently drawn attention of environmental scientists. In 2008, NETL researchers observed that CO_2 molecules may permanently intercalate between the clay lamellae (Romanov and Soong, 2008) and suggested a sorption mechanism akin to nano-confinement (Romanov et al., 2009a); independently, Busch et al. (2008) conducted experiments on well-characterized shale samples (Muderong Shale, Australia) and reported a relatively high CO_2 sorption capacity compared to coal as well as poor reproducibility in repeat experiments on the same samples, which they attributed to strong CO_2 interaction with clay minerals present in the shale. Romanov et al. (2009b) reported irreversible swelling of Ca-smectite after exposure to CO_2 in prolonged pressure build-up experiments, with preliminary results suggesting a subsequent carbonate formation in the interlayer region. The sorption of volatile fluids in swelling clay was further investigated using *ab initio* and classical simulations (Cygan et al., 2010; Botan et al., 2010; Cygan et al., 2012), which showed that the hydrated clay system is capable of sorbing linear CO_2 molecules via intercalation. The disposition of CO_2 molecules and density profiles of atoms within interlayer of Na-montmorillonite from molecular dynamics (MD) simulations (Cygan et al., 2012) are consistent with Monte Carlo simulations for lower CO_2 content (Botan et al., 2010). Comparison of the preliminary experimental and theoretical results presented by Romanov et al. (2010a) was followed by advanced complementary studies (Giesting et al., 2012a,b; Romanov et al., 2010b). It was reported that the modeling results and experimental observations indicate that sufficient presence of water species in the interlayer region is necessary for intercalation of CO_2 (Romanov et al., 2010b). The following X-ray diffraction (XRD) studies (Giesting et al., 2012a,b; Schaef et al., 2012; Ilton et al., 2012; Hemmen et al., 2012) focused primarily on changes in d_{001} basal spacing during and after the CO_2 treatment. The *in situ* (Giesting et al., 2012b) measurements replicating the pressure build-up experiments (Romanov et al., 2009b) confirmed the extent and irreversibility of matrix swelling observed *ex situ*. The reported XRD results indicate that the nature of the interlayer cations, degree of hydration, and the length of exposure to CO_2 can significantly affect the experimental outcome. However, the outcomes of these studies were inconsistent and specific nature of the CO_2-clay interactions governing this process was not fully understood. Among proposed mechanisms was formation of carbonate complexes that can be trapped in the interlayer via hydrogen bonding (Cole et al., 2010) or as part of the interlayer cation hydration shell (Giesting et al., 2012a).

The overall objective of this work was to develop a better understanding of the molecular interactions associated with CO_2 intercalation and the factors affecting CO_2 sorption in clay, especially the permanence of trapping, and to contribute to development of robust models for CO_2 storage in geologic reservoirs. Specific objectives were to conduct experimental investigation into the processes associated with CO_2 and H_2O trapped in swelling clays, namely, Wyoming and Texas montmorillonites, to provide evidence of the sorption mechanism via intercalation in the interlayer and to investigate the role of cation hydration as well as the longer-term changes in carbon dioxide bonding to the clay surfaces.

2. Materials and methods

2.1. Samples

The clay samples used in this work were SWy-2 (a low-charge Na^+-montmorillonite from Wyoming, with substitutions of Mg^{2+} and Fe^{2+} for Al^{3+} and minor substitutions of Al^{3+} for Si^{4+}, and the unit-cell structure: $(Ca_{0.12}Na_{0.32}K_{0.05})[Al_{3.01}Fe(III)_{0.41}Mn_{0.01}Mg_{0.54}Ti_{0.02}][Si_{7.98}Al_{0.02}]O_{20}(OH)_4)$; STx-1b (a low-iron Ca^{2+}-montmorillonite from Texas, with isomorphic substitutions in the octahedral sheet only and the unit-cell structure: $(Ca_{0.27}Na_{0.04}K_{0.01})[Al_{2.41}Fe(III)_{0.09}Mn_{tr}Mg_{0.71}Ti_{0.03}][Si_{8.00}]O_{20}(OH)_4)$; and SAz-2 (a heterogeneous high-charge Ca^{2+}-montmorillonite from Arizona, known as "Cheto," with isomorphic substitutions in the octahedral sheet only and the unit-cell structure: $(Ca_{0.39}Na_{0.36}K_{0.02})[Al_{2.71}Fe(III)_{0.12}Mn_{0.01}Mg_{1.11}Ti_{0.03}][Si_{8.00}]O_{20}(OH)_4)$ – which had been acquired from the Source Clays Repository, the Clay Minerals Society, Department of Geology, University of Missouri, Columbia, MO (Martin, 1979) and were used as received except when it is stated otherwise. The SWy-2 and STx-1b were received in form of powder and SAz-2 was received as natural lumps. Control experiments on the lumps were used to verify significance of the findings for similar clay powders.

2.2. Sorption isotherms

We used the NETL-built manometric apparatus (Romanov et al., 2006), to measure CO_2 (99.999% purity, Valley Co., Pittsburgh, PA, USA) sorption as a function of pressure and temperature swings. The gases were pressurized by the ISCO syringe pump (Model 500D). In the first test, SWy-2 and STx-1b powders were loaded into separate sample cells and then the sample and reference cells' void volumes were determined with estimated accuracy of 0.1 cm^3 by repeatedly injecting helium (99.997% purity, Valley Co., Pittsburgh, PA, USA). Evacuation of the system was done by the Edwards high-vacuum pump (Model E2M8) at 55 °C, for 2–3 days prior to the tests to remove non-bound water. Temperature was varied during the test and stabilized with accuracy of 0.1 °C, by the VWR refrigerated bath circulator (Scientific Products, Model 1196). Standard calibration and statistical correlation techniques were used to account for the non-equilibrium test conditions, including the temperature corrections to the pressure transducer readings (Romanov et al., 2006).

The initial part of the test was a standard CO_2 sorption isotherm (55 °C, up to 7 MPa) on as-received SWy-2 and STx-1b powders, with at least two-hour equilibration at each pressure, for a total of 8 h. The samples were subsequently heated to above 90 °C, with the closed-volume CO_2 pressure increasing above 10 MPa, then cooled to 55 °C and slowly depressurized to determine residual sorption.

For comparison of the powder data with natural clay, the as-received SAz-2 lump sample was tested using the same protocol as in the above experiments on SWy-2 and STx-1b but with longer steps at each pressure (2–3 days) at 55 °C to allow for potentially slower equilibration of the large lumps compared to powder. The SAz-2 sample was subsequently exposed to supercritical CO_2 (at 10.5 MPa and 90 °C), for 10 minutes and slowly decompressed. The SAz-2 lump was crushed and ground into powder only after being exposed to CO_2 in order to prepare it for the Fourier-transform Infrared (FTIR) studies.

Eight months later, the CO_2 sorption isotherms have been repeated on the SWy-2 and STx-1b powders moisture-equilibrated under the room conditions of <20% relative humidity (RH). These tests were done in two runs each, with relatively short (for a total exposure of 4 h) and long (for a total exposure of 10 days) equilibration times.

2.3. Infrared spectroscopy

Diffuse reflectance infrared spectra were collected using the FTIR spectrometer (Thermo Electron Corporation, Model Nicolet 4700) with liquid nitrogen-cooled HgCdTe (MCT) detector and a Smart Collector with dual environmental chamber equipped with ZnSe windows. House nitrogen purge was used to reduce infrared absorption in the air CO_2. The studied clay powder samples (<200 mg) were randomly mounted in the sample compartment and the control sample (powder of the corresponding original, as-received clay) was mounted in the interconnected reference cell. Before being placed inside the environmental chamber, all SAz-2 lumps, either as-received or after the prior exposure to CO_2, were slowly and gently ground into powder while taking care to prevent overheating of the clay particles caused by friction.

To avoid higher MCT detector noise as well as interference effects created by variable particle size, the collected spectrum was limited to 4000–500 cm^{-1} in the middle-IR (MIR) range. In each measurement, at least 256 scans were done with 2 cm^{-1} resolution. The spectra of the as-received clays were used for background subtraction. To monitor long-term spectral changes, the samples of SWy-2 and STx-1b clays exposed to CO_2 were left in the dual-chamber compartments for eight months to ensure that the same area was repeatedly scanned.

2.4. X-ray diffraction

The X-ray diffraction (XRD) patterns were produced on randomly oriented clay powder samples using a multi-purpose diffractometer X'Pert PRO MPD (PANalytical, B.V., Almelo, The Netherlands) with a Cu X-ray source operated at 45 kV and 40 mA and an X'Celerator detector equipped with a monochromator. Data were collected from 3 to 60°2θ using a step size of 0.02°2θ and a count time of at least 2 s per step, immediately (within 15 min) after several trials of CO_2 exposure of the clay samples in manometric apparatus, including the above mentioned sorption isotherm experiments on as-received clay samples as well as short (4 h) and long (10 days) additional exposures of the identical clay samples that were allowed to sit open under room conditions, 21 °C and <20% RH, for eight months before the experiments. The sample transfer was done in dry-nitrogen-filled vessels. Each time, the same day and under the same ambient conditions, a control run was done with the identical clay samples that were not exposed to CO_2.

3. Results and discussion

3.1. CO_2 sorption isotherms

NIST Pure Fluids (Lemmon et al., 2000), Database 12, ver. 5.0 was used to calculate the equation-of-state (EOS) for CO_2. Reproducibility of the derived sorption isotherm data is poor with respect to the exact amount of residual sorption (Busch et al., 2008; Romanov et al., 2010b) but the sorption–desorption hysteresis during the isothermal (55 °C) portion of the test, shown for the 20% RH-equilibrated samples and long CO_2-equilibration times (Fig. 1), was observed to varying extents (Romanov et al., 2009b) except for sorption on the clay powder dried by heating in vacuum prior to the tests. The data for the as-received samples and for shorter equilibration times are similar but are not shown here due to larger errors associated with the EOS uncertainties. Despite the relatively low accuracy of such measurements, it is worth mentioning that the residual sorption correlated with apparent *in situ* swelling of the clay minerals at high CO_2 pressures, evidenced by the negative slope (Cygan et al., 2012) of the sorption isotherm plots. To test the hypothesis of the residual CO_2 trapping further, direct measurements of the sample weight change caused by exposure to CO_2 were completed on the same samples. The measured weight gain (up to +0.3% for SWy-2 and +0.4% for STx-1b) was much smaller than the weight gain that would correspond (in the excess de-sorption plots, without accounting for clay dehydration) to the residual sorbed amount of CO_2. Hence one can infer that at least some interlayer water has been displaced by the CO_2 molecules.

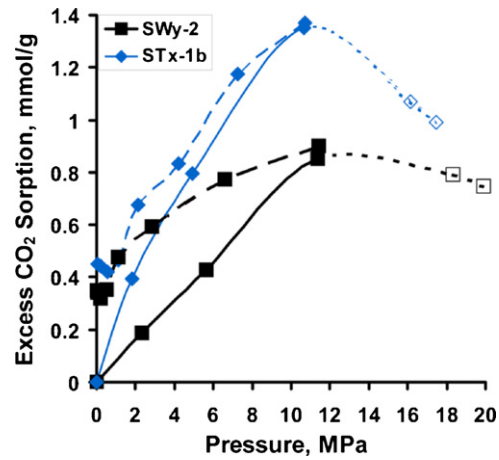

Fig. 1. Excess CO_2 sorption isotherms: solid lines (—) at 55 °C; dotted lines (. . .) at >90 °C; dashed lines (- - -) for decompression (desorption).

Assuming that inter-particle voids inaccessible to helium can be neglected and that the dry-mineral grain density (Holmboe et al., 2012; Lutterotti et al., 2010) is 2.8 g/cm^3 for SWy-2 and 3.1 g/cm^3 for STx-1b, the *in situ* helium pycnometry data of grain density >2.3 g/cm^3 for all SWy-2 and >2.2 g/cm^3 for all STx-1b samples correspond to water contents of <0.08 g-H_2O/g-clay for SWy-2 and <0.18 g-H_2O/g-clay for STx-1b, which indicates that SWy-2 had an incomplete monolayer of interlayer water or, most likely, interstratified 0 and 1 interlayer water (0–1 W) layers and STx-1b had 1–2 W layers. These numbers are consistent with 15–30% RH equilibration conditions (Ferrage et al., 2005).

The sorption isotherm data show that CO_2 sorption capacity of the montmorillonite powder is comparable to sorption capacity of coal. The control experiment with CO_2 sorption on SAz-2 lumps resulted in the excess sorption plots (not shown) similar to the STx-1b, which indicates that low permeability of the natural (not powdered) clay deposits may not be an issue if they are sufficiently dry.

3.2. Diffuse reflectance infrared Fourier-transform spectroscopy (DRIFTS)

The infrared spectroscopy was used to verify the permanence of CO_2 trapping indicated by the manometric results. The diffuse reflectance spectra provided further evidence that CO_2 enters the interlayer and becomes trapped there for at least several months under the ambient conditions. The following FTIR studies have primarily focused on antisymmetric (asymmetric) stretching (ν_3) and bending (ν_2) vibrations of the residual CO_2 molecules (Fig. 2) that remain trapped in Wyoming (SWy-2) and Texas (STx-1b) montmorillonite powder several months after exposure to supercritical carbon dioxide.

The observed vibrational frequency (ν_3^*) shifts (see Supplementary data) were stable over a period of eight months, highly reproducible for both of these montmorillonites and independent of their hydration state, −5 cm^{-1} for SWy-2 and −10 cm^{-1} for STx-1b; but the IR-active 'trapped CO_2' modes were not as readily detected in the similarly treated samples of Arizona

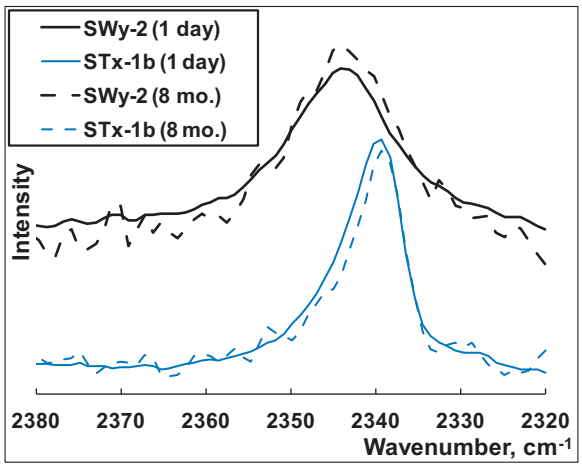

Fig. 2. FTIR spectra after exposure to CO_2: solid lines (—) within 24 h; dashed lines (- - -) for same samples 8 months later (5× magnification).

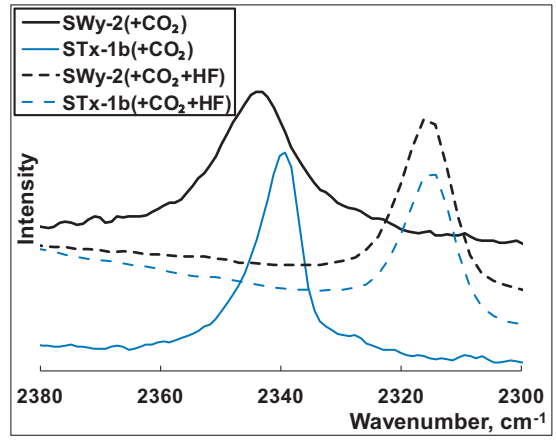

Fig. 4. FTIR spectra after exposure to CO_2: solid lines (—) within 24 h; dashed lines (- - -) for residue of the same CO_2-exposed samples after subsequent HF acid digestion.

(SAz-2) montmorillonite (see Supplementary data). These frequency shifts are significant to indicate some form of physical trapping, yet too small to suggest strong chemical bonding for these CO_2 moieties. However, in the long term, the significant drop in the ν_3^* intensity may indicate some ongoing chemical processes such as carbonation.

It appears that an apparent carbonate band near 1430 cm^{-1} has significantly increased in intensity over time in the SWy-2 sample, several months after exposure to CO_2 (Fig. 3). A sharp peak observed at 1475 cm^{-1} has not been properly identified but it can be tentatively attributed to either a regularly structured form of a carbonate (mineralization) or aromatic C=C stretching vibrations.

Barring the chemisorption, persistence of the 'trapped CO_2' vibrations in SWy-2 and STx-1b after the decompression is an evidence of extreme (molecular or nano-scale) confinement that prevents some of the CO_2 molecules from diffusing out of molecular-scale traps, presumably located in the interlayer region. The term nano-confinement is introduced here to distinguish this molecular-scale trapping mechanism from reversible physical sorption in micropores, with diameters <2 nm as defined in the IUPAC guidelines on reporting physisorption data (Sing et al., 1985).

As a proof that the initial irreversible trapping of CO_2 molecules is not due to chemical bonding, boiling of the clay samples in hydrofluoric acid (HF) at 250 °C (in a failed attempt to chemically release the 'trapped CO_2') did not affect the magnitude of the signal but shifted the ν_3^* peaks in both clays to the same frequency, 2315 cm^{-1} (Fig. 4), which fits the red-shift trend for asymmetric-stretch vibrational frequencies of the matrix isolated CO_2 halide anions (Weber and Schneider, 2004). The CO_2 fluoride peak sits on the right shoulder of a much broader absorption band (see Supplementary data) which is tentatively assigned to complex molecular lattice bands in combination with CO_2 asymmetric stretching (Palmer et al., 1981; Roux et al., 1979). Since the nano-confined CO_2 does not appear to be chemically released until complete destruction of the clay matrix, the standard CO_2 coulometer test cannot be used to accurately quantify the amount of carbon dioxide trapped in the interlayer.

No distinct CO_2 bending-mode vibrations (ν_2^*) were observed, in excess of background, in the montmorillonite samples either immediately after their exposure to CO_2 or several months later (see Supplementary data), which is another indication of the extreme quantum confinement.

3.3. XRD patterns

Original (as received) clay samples had significant amount of cation hydration in the interlayer, which is shown in relatively large basal spacing, d_{001} (Fig. 5) corresponding to the (0 0 1) Bragg reflections, a broader (2θ FWHM~3°) one-monolayer-hydrate peak (12.2 Å) for Na-montmorillonite and a narrower

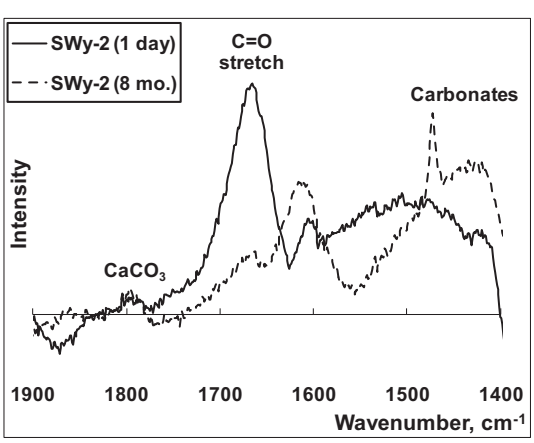

Fig. 3. FTIR spectra after exposure to CO_2: solid line (—) within 24 h; dashed line (- - -) for the same sample 8 months later.

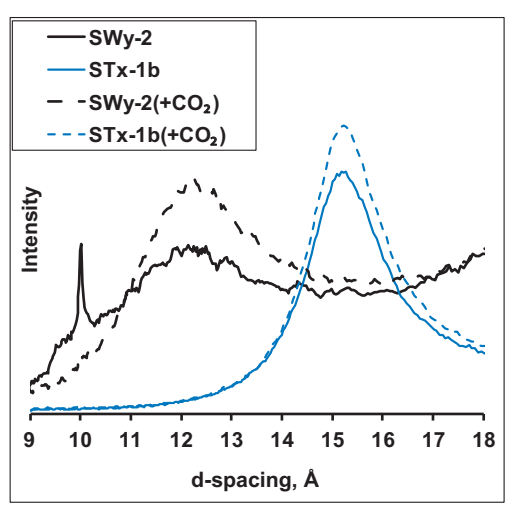

Fig. 5. XRD patterns: solid lines (—) for 'as-received' samples; dashed lines (- - -) after 10 MPa CO_2.

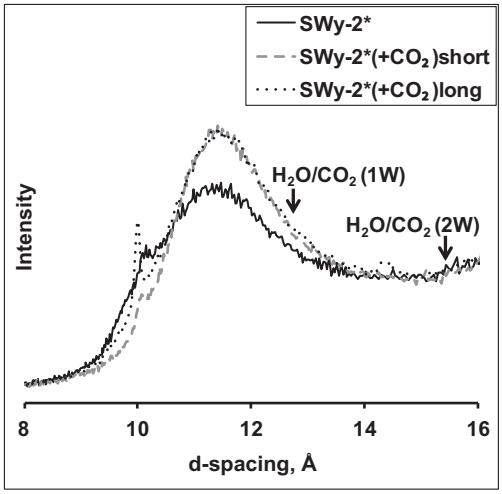

Fig. 6. XRD patterns of SWy-2 after equilibration under <20% RH (*): solid line (—) before CO_2; dashed line (- - -) after the 4-h CO_2 test; dotted line (. . .) after the 10-day CO_2 test.

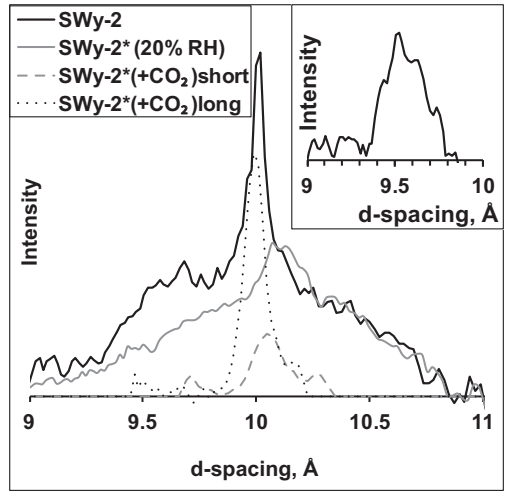

Fig. 7. XRD patterns of 'as-received' SWy-2, solid black line (—), with isolated shoulder band shown in the inset; and SWy-2 after <20% RH equilibration (*), solid gray line (—) before exposure to CO_2, dashed line (- - -) after 4-h CO_2, dotted line (. . .) after 10-day CO_2 exposure.

(2θ FWHM~0.7°) two-monolayer-hydrate peak (15.2 Å) for Ca-montmorillonite. After exposure to supercritical CO_2, the main d_{001} peaks become narrower (by >30% in Na-montmorillonite and by <3% in Ca-montmorillonite), suggestive of slightly decreased hydration heterogeneity and/or higher degree of stacking in the elementary tactoids (quasi-crystals). A prominent feature ($d_{001} \sim 10$ Å) representing nearly collapsed interlayers in the 'as-received' Na-montmorillonite had almost completely disappeared after exposure to CO_2 (Fig. 5).

As both 'as-received' samples were allowed to sit open under room conditions, 21 °C and <20% RH (labeled with *), the main XRD peaks have gradually shifted to lower *d*-spacing values but the nearly-collapsed interlayer feature in SWy-2* has broadened and shifted to a slightly higher (10.1 Å) value (Fig. 6). Still, the Ca-montmorillonite samples appeared to be more homogeneously hydrated (2θ FWHM~1.2°) than the Na-montmorillonite (2θ FWHM~2°). Both 20%-RH clays were subjected to two CO_2 sorption experiments similar to the initial sorption test. In the first (short) experiment, the exposure to CO_2 was 4 h; the exposure in the subsequent (long) experiment was 10 days. In case of SWy-2*, the main XRD peak (11.4 Å) behaved the same way as with the original, 'as-received' sample: it increased in intensity while becoming slightly narrower (Fig. 6).

Similarly, exposure to CO_2 has removed the broader wings (9–11 Å) around the sharper features at 10.0–10.1 Å, in all instances; the feature at 9.55 Å (Fig. 7, inset) attributed to the completely collapsed interlayer of a pure Na-montmorillonite[4] was significant only in 'as-received' SWy-2. The apparent hydration heterogeneity of the SWy-2* after the long exposure to CO_2 almost replicated that of the more hydrated 'as-received' SWy-2 prior to CO_2 treatment: both samples had distinct features at 10.0 Å and 14.4 Å; but the main reflection peak of the SWy-2* clay after the CO_2 exposure became narrower (2θ FWHM = 1.4°) and did not shift vs. the SWy-2* prior to CO_2 treatment. These features were present in 'as-received' SWy-2 only before exposure to CO_2 (but not in SWy-2* before exposure to CO_2) and were found in SWy-2* only after the long (but not after the short) exposure to CO_2 (Fig. 7). The higher-order reflections of the SWy-2 samples were similar to each other (see Supplementary data) and did not reveal strong correlations. This suggests that CO_2 interaction with such heterogeneous clays is very complex and may result in either swelling or drying and shrinking of certain interlayer galleries, depending on yet unidentified factors that govern the mixing kinetics of the CO_2-H_2O systems.

While the 'as-received' and the 20%-RH Na-montmorillonites are both representative of a partly-filled first hydrate-monolayer, the 'as-received' and the 20%-RH Ca-montmorillonites are the extreme cases of the nearly-filled ($d_{001} \sim 15.2$ Å) and the marginally-opened but effectively vacant ($d_{001} \sim 13.1$ Å) second monolayer respectively. After exposure to CO_2 the basal repeat distances of the 20%-RH STx-1b (STx-1b*) consistently increased by ~1.1 Å (Fig. 8), in both short and long experiments that were completed about 10 days apart, with the control STx-1b* sample run the same day each time. The higher-order reflections have changed as well (see Supplementary data). Since, during the experiment, every effort was made to eliminate the residual micropore water (drying in vacuum, heating above 90 °C, and pressure cycling with high purity CO_2), the increase in d_{001} should be attributed to CO_2 penetration into the lattice spacings (via intercalation) rather than to formation of a second hydrate layer between the strata. The partial irreversibility of the CO_2 intercalation observed on the same

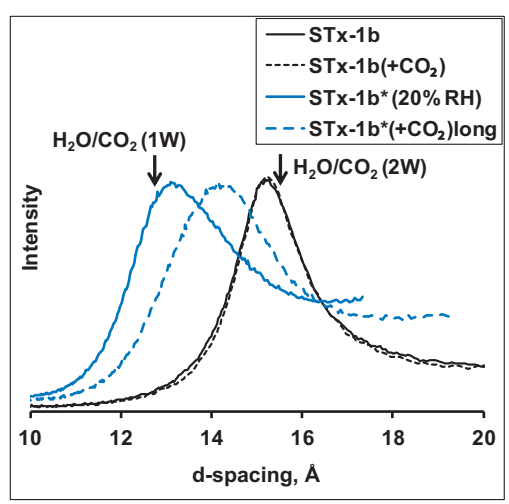

Fig. 8. XRD patterns: black line (—) for 'as-received' STx-1b sample; blue line (——) for STx-1b after <20% RH (*); dashed lines (- - -, — — —) for after 10 MPa CO_2 (scaled). (For interpretation of the references to color in this figure legend, the reader is referred to the web version of the article.)

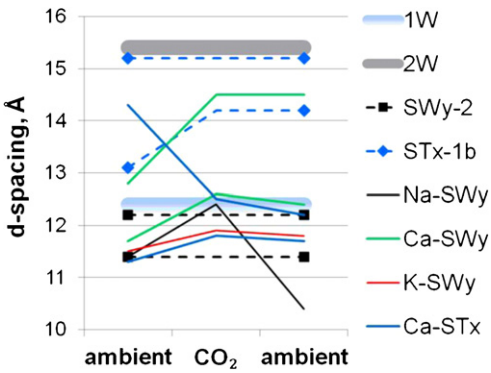

Fig. 9. Chronological d001 changes in SWy-2 and STx-1b (Romanov et al., 2009b), before and after the exposure to sc-CO_2 and then after outgassing (ambient) vs. references: Na-SWy-2 (Giesting et al., 2012a), Ca-SWy-2 (Giesting et al., 2012b), K-SWy-2 (Giesting et al., 2012b), Ca-STx-1b (Schaef et al., 2012), 1W state (Cygan et al., 2004), and 2W state (Cygan et al., 2004).

samples as the sorption hystheresis and the IR spectra supports the hypothesis of nano-confinement within interlayer or, at least partly, within adjacent structural cavities.

The difference between the long- and short-term exposure to CO_2 (not shown) was minor and indicated that only 5% of the platelets (with an average d-spacing of ~13.3 Å) still continued to expand by ~1.1 Å into the platelets with an average d-spacing of ~14.4 Å, beyond the first four hours of exposure, thus indicating that CO_2 penetrates into such structures (with greater H_2O/CO_2 population) much slower than into the ones with the minimal amount of hydration necessary to prop open the second monolayer. The incremental long-term expansion, +0.2 Å was on the same scale as in the (ultimately, irreversible) *in situ* kinetics experiments (Giesting et al., 2012b). Incidently, the main peak in STx-1b* shifts toward the same position (14.4 Å) as the secondary peak in SWy-2*, both after the long exposure to CO_2 and under the same atmospheric conditions (Fig. 6).

These d-spacing data for both SWy-2 and STx-1b samples were also compared to the *in situ* literature data (Fig. 9). Notably, the Na-montmorillonite with partly filled (sufficiently open) first hydrate monolayer appears to swell by up to ~1 Å, allowing CO_2 to completely fill the first monolayer at pressures above 5 MPa, and then shrink (after the short, 10 min. exposure to CO_2), upon decompression, below the initial d-spacing (Giesting et al., 2012a) as the CO_2 apparently displaces the water molecules in the interlayer (Fig. 9). However, Giesting et al. (2012a) reported no swelling for Na-SWy samples either with initial d_{001} < 10 Å or with a completely filled first hydrate monolayer, d_{001} = 12.3–12.5 Å. Similar types of swelling behavior were reported for the K-SWy (Giesting et al., 2012b), Ca-SWy (Giesting et al., 2012b), and some Ca-STx (Schaef et al., 2012) samples in 0–1 W hydration state (Fig. 9).

Both Romanov et al. (2009b) and Giesting et al. (2012b) observed irreversible swelling up to 15–15.5 Å in the long-term pressure build-up experiments with Ca-smectites in 1–2 W hydration state, which suggests some reorganization of the interlayer content (Giesting et al., 2012b) that increases stability of the CO_2-clay system over time; but Schaef et al. (2012) reported only shrinking, attributed to drying effects of high-pressure CO_2, for the Ca-STx samples with partly filled second hydrate layer and initial d_{001} > 13 Å (Fig. 9). One possible explanation for the lack of consistency in these data is importance of the differences in dynamic application of the CO_2 pressure that result in various degrees of CO_2-H_2O mixing in the interlayer as opposed to sheer mechanical displacement of H_2O molecules by the high-pressure CO_2 flow. As was demonstrated by Hemmen et al. (2012) for the synthetic Na-smectite, the rate of CO_2 intercalation can be very slow compared to the interlayer mobility of water species that is facilitated by osmotic swelling of the clay matrix (van Olphen, 1963). Giesting et al. (2012b) observed that the kinetics differ significantly depending on the nature of interlayer cation, with Ca-exchanged montmorillonite swelling more slowly.

4. Conclusions

The results of this work show that natural montmorillonite has significant sorption capacity to carbon dioxide that can be trapped in the interlayer region. The interlayer CO_2 may cause an irreversible expansion of clay depending on the degree of the cation hydration and the dynamic application of the CO_2 pressure, which results in CO_2-H_2O mixing in the interlayer as opposed to displacement of H_2O by CO_2 flow. The FTIR spectra indicate that the initially loosely bound CO_2 molecules between the strata eventually chemically react with alkaline cations under the ambient conditions. The corroborated results of several techniques (manometric sorption, IR, XRD, and chemical digestion) simultaneously applied to the same clay samples provide conclusive evidence that CO_2 molecules may permanently intercalate between the lamellae and suggests the initial sorption mechanism akin to that of the nano-confinement. The 'trapped CO_2' is accessible to HF but the resulting nano-confined CO_2:F adducts are not extractable.

Acknowledgements

The author appreciates assistance with XRD characterization provided by Elizabeth Frommell as well as discussions of the technical approach with Bret Howard at the National Energy Technology Laboratory. This research was supported in part by an appointment to the U.S. Department of Energy (DOE) Postgraduate Research Program at the National Energy Technology Laboratory administered by the Oak Ridge Institute for Science and Education under the RDS contract DE-AC26-04NT41817.

Appendix A. Supplementary data

Supplementary data associated with this article can be found, in the online version, at http://dx.doi.org/10.1016/j.ijggc.2013.01.022.

References

Aylmore, L.A.G., Sills, I.D., Quirk, J.P., 1970. Surface area of homoionic illite and montmorillonite clay minerals as measured by the sorption of nitrogen and carbon dioxide. Clays and Clay Minerals 18 (2), 91–96.

Botan, A., Rotenberg, B., Marry, V., Turq, P., Noetinger, B., 2010. Carbon dioxide in montmorillonite clay hydrates: thermodynamics, structure, and transport from molecular simulation. The Journal of Physical Chemistry C 114 (35), 14962–14969.

Brunauer, S., Emmett, P.H., Teller, E., 1938. Adsorption of gases in multimolecular layers. Journal of the American Chemical Society 60 (2), 309–319.

Busch, A., Alles, S., Gensterblum, Y., Prinz, D., Dewhurst, D.N., Raven, M.D., Stanjek, H., Krooss, B.M., 2008. Carbon dioxide storage potential of shales. International Journal of Greenhouse Gas Control 2 (3), 297–308.

Cole, D.R., Chialvo, A.A., Rother, G., Vlcek, L., Cummings, P.T., 2010. Supercritical fluid behavior at nanoscale interfaces: implications for CO_2 sequestration in geologic formations. Philosophical Magazine 90 (17), 2339–2363.

Cygan, R.T., Liang, J.-J., Kalinichev, A.G., 2004. Molecular models of hydroxide, oxyhydroxide, and clay phases and the development of a general force field. Journal of Physical Chemistry B 108 (4), 1255–1266.

Cygan, R.T., Romanov, V.N., Myshakin, E.M., 2010. Natural materials for carbon capture. Sandia report; SAND2010-7217. Sandia National Laboratories, U.S. Department of Energy, Albuquerque, NM, and references therein.

Cygan, R.T., Romanov, V.N., Myshakin, E.M., 2012. Molecular simulation of carbon dioxide capture by montmorillonite using an accurate and flexible force field. Journal of Physical Chemistry C 116 (24), 13079–13091.

DOE/NETL, 2010. Carbon Dioxide Capture and Storage RD&D Roadmap; Roadmap. National Energy Technology Laboratory, U.S. Department of Energy Office of Fossil Energy, Washington, DC http://www.netl.doe.gov/technologies/carbon_seq/refshelf/CCSRoadmap.pdf

Fahmy, T.M., Paulaitis, M.E., Johnson, D.M., McNally, M.E.P., 1993. Modifier effects in the supercritical fluid extraction of solutes from clay, soil, and plant materials. Analytical Chemistry 65 (10), 1462–1469.

Ferrage, E., Lanson, B., Sakharov, B.A., Drits, V.A., 2005. Investigation of smectite hydration properties by modeling experimental X-ray diffraction patterns: Part I. Montmorillonite hydration properties. American Mineralogist 90 (8-9), 1358–1374.

Fripiat, J.J., Cruz, M.I., Bohor, B.F., Thomas Jr., J., 1974. Interlamellar adsorption of carbon dioxide by smectites. Clays and Clay Minerals 22 (1), 23–30.

Giesting, P., Guggenheim, S., Koster van Groos, A.F., Busch, A., 2012a. Interaction of carbon dioxide with Na-exchanged montmorillonite at pressures to 640 bars: implications for CO_2 sequestration. International Journal of Greenhouse Gas Control 8, 73–81.

Giesting, P., Guggenheim, S., Koster van Groos, A.F., Busch, A., 2012b. X-ray diffraction study of K- and Ca-exchanged montmorillonites in CO_2 atmospheres. Environmental Science and Technology 46 (10), 5623–5630.

Hemmen, H., Rolseth, E.G., Fonseca, D.M., Hansen, E.L., Fossum, J.O., Plivelic, T.S., 2012. X-ray studies of carbon dioxide intercalation in sodium fluorohectorite clay at near-ambient conditions. Langmuir 28 (3), 1678–1682, and references therein.

Holmboe, M., Wold, S., Jonsson, M., 2012. Porosity investigation of compacted bentonite using XRD profile modeling. Journal of Contaminant Hydrology 128 (1-4), 19–32.

Ilton, E.S., Schaef, H.T., Qafoku, O., Rosso, K.M., Felmy, A.R., 2012. In situ X-ray diffraction study of Na^+ saturated montmorillonite exposed to variably wet super critical CO_2. Environmental Science & Technology 46 (7), 4241–4248.

Knudson Jr., M.I., McAtee Jr., J.L., 1973. Interlamellar and multilayer nitrogen sorption by homoionic montmorillonites. Clays and Clay Minerals 22 (1), 59–70.

Lemmon, E.W., Peskin, A.P., McLinden, M.O., Friend, D.G., 2000. NIST Thermodynamic and Transport Properties of Pure Fluids – NIST Pure Fluids. NIST, U.S. Department of Commerce, Gaithersburg, MD.

Lutterotti, L., Voltolini, M., Wank, H.-R., Bandyopadhyay, K., Vanorio, T., 2010. Texture analysis of a turbostratically disordered Ca-montmorillonite. American Mineralogist 95 (1), 98–103.

Martin, R.T., 1979. In: van Olphen, H., Fripiat, J.J. (Eds.), Data Handbook for Clay Materials and Other Non-Metallic Minerals. Pergamon Press/Oxford, Elmsford, New York, NY.

Palmer, K.F., Wood, B.E., Roux, J.A., 1981. Infrared Optical Properties of Solid Mixtures of Molecular Species at 20°K; AEDC-TR-80-30 (ADA094214). Arnold Engineering Development Center, U.S. Air Force, Tennessee.

Romanov, V., Soong, Y., Schroeder, K., 2006. Volumetric effects in coal sorption capacity measurements. Chemical Engineering and Technology 29 (3), 368–374.

Romanov, V., Soong, Y., 2008. Multi-scale modeling of carbon dioxide sequestration in unmineable coal seams. In: 7th Ann. Conf. Carbon Capture & Sequestration, Pittsburgh, PA.

Romanov, V.N., Ackman, T.E., Soong, Y., Kleinman, R.L., 2009a. CO_2 storage in shallow underground and surface coal mines: Challenges and opportunities. Environmental Science & Technology 43 (3), 561–564, and references therein.

Romanov, V.N., Soong, Y., Howard, B.H., Frommell, E.A., Kleinmann, R.L., Guthrie, G.D., 2009b. CO_2 trapping in clayey materials. In: 46th Ann Meeting of the Clay Minerals Society, Billings, MT.

Romanov, V.N., Cygan, R.T., Howard, B.H., Myshakin, E.M., Guthrie, G.D., 2010a. Mechanisms of CO_2 interaction with expansive clay. In: Proc. SEA-CSSJ-CMS Trilateral Meeting on Clays, Seville, Spain, p. 228.

Romanov, V.N., Howard, B.H., Lynn, R.J., Warzinski, R.P., Hur, T.B., Myshakin, E.M., Lopano, C.L., Voora, V.K., Al-Saidi, W.A., Jordan, K.D., Cygan, R.T., Guthrie, G.D., 2010b. CO_2 interaction with geomaterials (Invited). In: American Geophysical Union, Fall Meeting, San Francisco, CA, p. H11J-01.

Roux, J.A., Wood, B.E., Smith, A.M., 1979. IR Optical Properties of Thin H_2O, NH_3, and CO_2 Cryofilms; AEDC-TR-79-57 (ADA074913). Arnold Engineering Development Center, U.S. Air Force: Tennessee.

Schaef, H.T., Ilton, E.S., Qafoku, O., Martin, P.F., Felmy, A.R., Rosso, K.M., 2012. In situ XRD study of Ca^{2+} saturated montmorillonite (STX-1) exposed to anhydrous and wet supercritical carbon dioxide. International Journal of Greenhouse Gas Control 6, 220–229.

Sing, K.S.W., Everett, D.H., Haul, R.A.W., Moscou, L., Pierotti, R.A., Rouquerol, J., Siemieniewska, T., 1985. Reporting physisorption data for gas/solid systems: with special reference to the determination of surface area and porosity (Recommendations 1984). Pure & Applied Chemistry 57 (4), 603–619.

Thomas Jr., J., Bohor, B.F., 1968. Surface area of montmorillonite from the dynamic sorption of nitrogen and carbon dioxide. Clays and Clay Minerals 16 (1), 83–91.

Thomas Jr., J., Bohor, B.F., Frost, R.F., 1970. Letters to the editor: surface area measurements on clays. Clays and Clay Minerals 18 (6), 405–409.

van Olphen, H., 1963. An Introduction to Clay Colloid Chemistry. Interscience Publishers, John Wiley & Sons, New York, NY.

Weber, J.M., Schneider, H., 2004. Infrared spectra of $X^- \cdot CO_2 \cdot Ar$ cluster anions (X=Cl, Br, I). The Journal of Chemical Physics 120 (21), 10056–10061, and references therein.